Pergamon

Int. J. Solids Structures Vol. 31, No. 23, pp. 3217–3231, 1994

0020–7683/94 $7.00 + .00

0020–7683(94)00083–2

FORMULATION OF THERMO-MECHANICAL FRICTIONAL CONTACT BASED ON COMPLEMENTARITY RELATIONS

JUN PARK and BYUNG MAN KWAK†
Department of Mechanical Engineering, Korea Advanced Institute of Science and Technology, 373-1 Kusong-dong, Yusong-gu, Taejon, 305-701, Korea

(*Received* 24 *August* 1993 ; *in revised form* 2 *May* 1994)

Abstract—On the basis of a linear complementarity, a mathematical formulation of thermo-mechanical frictional contact is presented. Depending on the status of contact, either a conduction condition or an insulation condition is applied. A complementarity condition between heat flow and temperature difference along the contact surface is found assuming that no thermal contact resistance exists. This thermal complementarity condition is implicitly related with the mechanical one. The resulting linear complementarity with additional constraints is solved by a modified Lemke's algorithm. Two numerical examples are presented to illustrate the procedure and solution behaviors.

INTRODUCTION

The analysis of thermo-mechanical contact can be important in many multidisciplinary mechanical engineering fields such as semi-conductors and electronic devices. It is complicated due to the coupling between mechanical and thermal fields. In the so-called zigzag approach (Montmitonnet *et al.*, 1992), the two fields are solved alternatively. The reduced rate of convergence with this method can be compensated for by the use of a symmetric solver. In the direct coupled formulation (Carter and Booker, 1989), however, an unsymmetrical stiffness matrix occurs. In the simple case of a steady-state heat transfer analysis, the effect of the mechanical field on the thermal can be neglected because heat generation and dissipation due to mechanical deformations are often negligible.

As compared to much interest in mechanical contact, little literature is available on the thermo-mechanical contact. Solution approaches of the mechanical contact can be divided into two categories: trial and error type iterative methods (Chandrasekaran *et al.*, 1987) and reformulations in terms of equivalent mathematical problem forms such as a variational inequality (Duvant and Lions, 1976; Panagiotopoulos, 1975, 1985; Antes and Panagiotopoulos, 1992) or a complementarity problem (Klarbring, 1986; Kwak and Lee, 1988; Kwak, 1990, 1991).

Available mathematical and numerical models of thermo-mechanical contact usually deal with conventional thermal boundary conditions (Comninou *et al.*, 1981; Panek and Dundurs, 1979; Mahmoud and El Shafei, 1989). This means that no resistance to heat flow in the contact region exists, while the bodies in the separated region do not exchange heat. In other words, the conventional boundary has a property of perfect contact or perfect insulation. In the actual thermo-mechanical contact region, however, there exists thermal contact resistance. Contact pressure and surface asperities are dominant parameters of thermal contact resistance (Holman, 1986). Thermal contact resistance rapidly decays asymptotically to zero as contact pressure increases. On the basis of the assumption that the contact surface is perfectly smooth, it can be neglected. Consequently, the temperature distribution and heat flux should be continuous across the contact surface.

In this paper, an analysis method is implemented for a two-dimensional thermo-mechanical frictional contact. Based on a linear complementarity of mechanical contact problem, a complementarity condition on thermal variables is appended. It adopts the

† To whom all correspondence should be addressed.

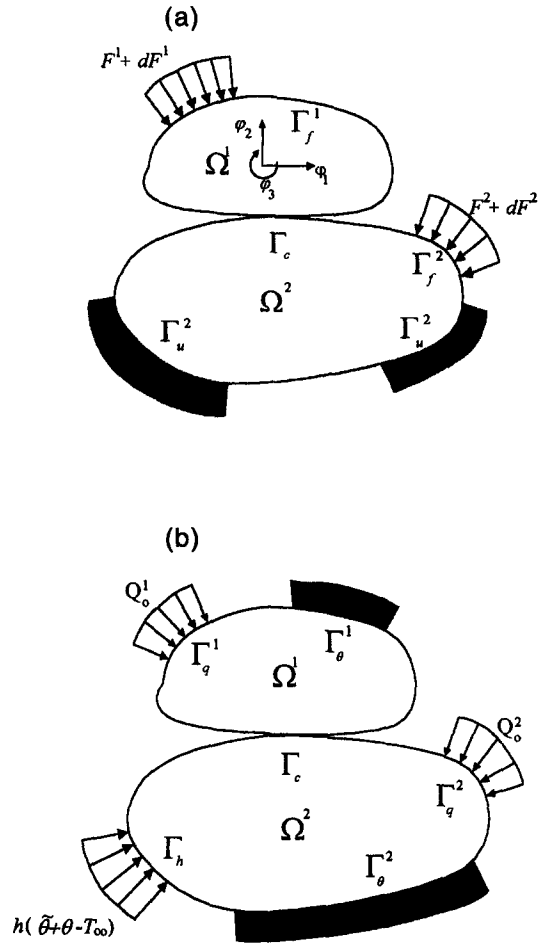

Fig. 1. Two bodies in contact with (a) mechanical, (b) thermal boundary conditions.

conventional thermal boundary concept and the Coulomb friction law. Two numerical examples are solved and the results of the examples compared with those by ABAQUS, a commercial FE code.

GOVERNING EQUATIONS

The two bodies in Fig. 1 are in a quasi-static equilibrium state mechanically and in a steady state thermally. Body 2 is assumed to be restrained against rigid body displacements. It is also assumed that heat transfer by radiation is neglected. The magnitude of heat transfer by conduction is much bigger than that by convection along the potential contact region.

Each boundary of the two bodies is composed of three disjoint parts mechanically; Γ_u where displacement is prescribed, Γ_f where traction boundary conditions are given and Γ_c which is the so-called potential contact region. Thermally, the boundary of each body is also divided into four disjoint parts; Γ_θ where temperature is given, Γ_h where heat transfer by convection occurs, Γ_q where heat flux condition is given and Γ_c where the conventional thermal boundary condition as explained above is applied.

(1) *Global equilibrium equation of body* 1

Body 1 is allowed to have rigid body motion φ as shown in Fig. 1, while body 2 is not. For body 1, all the external forces and the contact forces should be in equilibrium. The global equilibrium equation for body 1 is then obtained as follows:

$$\int_{\Gamma_f^j} (F_i + \mathrm{d}F_i)\mathbf{H}_{ij}\,\mathrm{d}\Gamma + \int_{\Gamma_c^j} (S_i + \mathrm{d}S_i)\mathbf{A}_{ij}\,\mathrm{d}\Gamma = 0, \tag{1}$$

where the coefficient matrix $\mathbf{H}_{ij}$ and $\mathbf{A}_{ij}$ represent the rigid body displacements of points of Γ_f and Γ_c in the ith coordinate direction due to a unit displacement in the jth rigid body degree of freedom φ_j, respectively. F_i and S_i denote traction vectors corresponding to the external and contact forces, respectively.

(2) *Local equilibrium equation of each body*

In the absence of body forces, the local equilibrium equation of each body is expressed as follows:

$$(\sigma_{ij}^k + \mathrm{d}\sigma_{ij}^k)_{,j} = 0 \quad \text{in}\,\Omega^k, \tag{2}$$

where the superscript k denotes body numbering.

(3) *Strain–displacement relation*

$$\mathrm{d}\varepsilon_{ij} = \tfrac{1}{2}(u_{i,j} + u_{j,i}), \tag{3}$$

where u is an increment of displacement during a load increment.

(4) *Stress and strain relation*

$$\mathrm{d}\sigma_{ij}^k = C_{ijlm}^k\,\mathrm{d}\varepsilon_{lm}^k - \beta_{ij}^k\theta, \tag{4}$$

where C_{ijlm}^k, β_{ij}^k and θ represent constitutive coefficients, thermal modulus and temperature change during a load increment, respectively.

(5) *Local heat equilibrium equation*

Assuming that heat generation or dissipation is neglected and considering a steady state, the local heat equilibrium equation is expressed as follows:

$$(q_i^k + \mathrm{d}q_i^k)_{,i} = 0 \quad \text{in}\,\Omega^k. \tag{5}$$

(6) *Heat flux–temperature relation*

It is the law of Fourier as follows:

$$\mathrm{d}q_i^k = -\kappa_{ij}^k\theta_{,j}, \tag{6}$$

where κ_{ij} means the coefficient of thermal conductivity.

(7) *Boundary conditions*

Mechanical boundary conditions are expressed as follows:

$$u_i = U_0 \quad \text{on}\,\Gamma_u^k, \tag{7}$$

$$(\sigma_{ij}^k + \mathrm{d}\sigma_{ij}^k)n_j^k = F_i^k + \mathrm{d}F_i^k \quad \text{on}\,\Gamma_f^k, \tag{8}$$

where U_0 is a given displacement increment and n is a unit normal vector.

Thermal boundary conditions are expressed as follows:

$$\theta = \vartheta_0 \quad \text{on } \Gamma_\theta^k, \tag{9}$$

$$(q_i + \mathrm{d}q_i)^k n_i^k = -Q_0 \quad \text{on } \Gamma_q^k, \tag{10}$$

$$(q_i + \mathrm{d}q_i)^k n_i^k = h[(\tilde{\theta} + \theta) - T_\infty] \quad \text{on } \Gamma_h^k, \tag{11}$$

where ϑ_0, Q_0, h and T_∞ are given, denoting temperature increment, heat flux, convection coefficient and ambient temperature, respectively. The temperature at the end of the previous thermal loading step is denoted by $\tilde{\theta}$.

(8) *Impenetration condition*

This is well described in Kwak (1991). Here only the resulting condition is summarized. The gap between two surfaces measured at a surface point a_i^1 after deformation can be represented as follows, in the first order approximation,

$$\mathbf{D}_n(a_i^1) = \mathbf{D}_n^0 - \mathbf{n}^{\mathrm{T}}(\mathbf{u}^1(a_i^1) + \mathbf{u}^2(a_i^2) + \mathbf{A}\boldsymbol{\varphi}), \tag{12}$$

where a_i^2 is the opposing contact point and $\mathbf{D}_n^0$ the initial gap before deformation occurs. The second term in the right-hand side of eqn (12) denotes displacement or separation due to pure deformation and rigid body displacement due to the rigid body degrees of freedom φ. Here $\mathbf{A}$ is the kinematic matrix representing the displacement of point a_i^1 due to φ as used in eqn (1).

Since either the contact gap $\mathbf{D}_n(a_i^1)$ or the corresponding contact normal force $\mathbf{P}$ between two mating contact points after load increment must be equal to zero, the following condition is also satisfied:

$$\mathbf{P} \cdot \mathbf{D}_n(a_i^1) = 0 \quad \text{for all } a_i^1 \text{ on } \Gamma_c^1. \tag{13}$$

(9) *Coulomb friction condition*

From the Coulomb friction law, the contact tangential force $\mathbf{S}_{\mathrm{T}}$ must satisfy the following relation:

$$-\mu\mathbf{P} \leqslant \mathbf{S}_{\mathrm{T}} \leqslant \mu\mathbf{P}, \tag{14}$$

where μ is the friction coefficient. If $|\mathbf{S}_{\mathrm{T}}| < \mu\mathbf{P}$, then there is no relative tangential displacement. If $|\mathbf{S}_{\mathrm{T}}| = \mu\mathbf{P}$, slip is imminent.

FINITE ELEMENT MODELING

The principle of virtual work for the mechanical part can be expressed as follows:

$$\int_V (\sigma_{ij} + \mathrm{d}\sigma_{ij})_{,j}\, \delta u_i \mathrm{d}V = 0, \tag{15}$$

where δu_i is a virtual displacement. For the sake of simplicity in notation, the superscript k which refers to the body numbering is omitted. By using Green's theorem and eqn (4), eqn (15) can be rearranged as,

$$\int_V C_{ijlm}\,\mathrm{d}\varepsilon_{lm}\delta\,\mathrm{d}\varepsilon_{ij}\,\mathrm{d}V-\int_V \theta\beta_{ij}\,\delta\,\mathrm{d}\varepsilon_{ij}\,\mathrm{d}V=\delta R-\int_V \sigma_{ij}\,\delta\,\mathrm{d}\varepsilon_{ij}\,\mathrm{d}V, \tag{16}$$

where δR denotes the external virtual work.

A similar variational equation for heat transfer can be expressed as follows:

$$\int_V (q_{i,i}+\mathrm{d}q_{i,i})\delta\theta\,\mathrm{d}V=0, \tag{17}$$

where $\delta\theta$ is a virtual temperature. Also by using Green's theorem and eqns (6), (9)–(11), this can be rewritten as follows:

$$\int_V \kappa_{ij}\,\theta_{,j}\,\delta\theta_{,i}\,\mathrm{d}V+\int_{\Gamma_h} h\theta\,\delta\theta\,\mathrm{d}\Gamma=\delta Q+\int_V q_i\,\delta\theta_{,i}\,\mathrm{d}V, \tag{18}$$

where

$$\delta Q=\int_{\Gamma_q} Q_0\delta\theta\,\mathrm{d}\Gamma+\int_{\Gamma_h} h(T_\infty-\tilde{\theta})\delta\theta\,\mathrm{d}\Gamma. \tag{19}$$

For the finite element discretization, each of the unknowns is approximated by appropriate shape functions with unknown parameters. The increment in displacement and temperature is then expressed as:

$$u=\mathbf{N}\mathbf{u}, \tag{20}$$

$$\theta=\mathbf{N}\boldsymbol{\theta}, \tag{21}$$

where $\mathbf{u}$ and $\boldsymbol{\theta}$ stand for the nodal displacement and temperature increment to be determined, respectively. $\mathbf{N}$ denotes shape functions. Then strain and heat flux can be approximated in terms of $\mathbf{u}$ and $\boldsymbol{\theta}$ as follows:

$$\mathrm{d}\varepsilon=\mathbf{B}_u\mathbf{u}, \tag{22}$$

$$\mathrm{d}q=\mathbf{B}_\theta\boldsymbol{\theta}, \tag{23}$$

where $\mathbf{B}_u$ and $\mathbf{B}_\theta$ are the strain–displacement transformation matrix and the temperature gradient interpolation matrix, respectively.

Following the usual finite element discretization procedure (Bathe, 1982), two matrix equations corresponding to eqns (16) and (18) are obtained. These equations can be combined as follows:

$$\begin{bmatrix}\mathbf{K}_{uu} & \mathbf{K}_{u\theta}\\ \mathbf{0} & \mathbf{K}_{\theta\theta}\end{bmatrix}\begin{Bmatrix}\mathbf{u}\\ \boldsymbol{\theta}\end{Bmatrix}=\begin{Bmatrix}R\\ Q\end{Bmatrix}-\begin{Bmatrix}\mathscr{R}\\ \mathscr{L}\end{Bmatrix}, \tag{24}$$

where

$$\mathbf{K}_{uu}=\int_V \mathbf{B}_u^{\mathrm{T}}\mathbf{C}\mathbf{B}_u\mathrm{d}V, \tag{25}$$

$$\mathbf{K}_{u\theta}=-\int_V \mathbf{B}_u^{\mathrm{T}}\boldsymbol{\beta}\mathbf{N}\,\mathrm{d}V, \tag{26}$$

$$\mathbf{K}_{\theta\theta} = \int_V \mathbf{B}_\theta^{\mathrm{T}} \boldsymbol{\kappa} \mathbf{B}_\theta \, \mathrm{d}V + \int_{\Gamma_h} h \mathbf{N}^{\mathrm{T}} \mathbf{N} \, \mathrm{d}\Gamma, \tag{27}$$

$$\mathscr{R} = \sum \int_V \mathbf{B}_u^{\mathrm{T}} \boldsymbol{\sigma} \, \mathrm{d}V, \tag{28}$$

$$\mathscr{L} = -\int_V \mathbf{B}_\theta^{\mathrm{T}} \mathbf{q} \, \mathrm{d}V, \tag{29}$$

and R and Q represent external force and heat flow, respectively.

Decomposing the nodal variables $\mathbf{u}$ and $\boldsymbol{\theta}$ into those on the potential contact region $\mathbf{u}^{\mathrm{c}}$ and $\boldsymbol{\theta}^{\mathrm{c}}$ and those on the interior $\mathbf{u}^{\mathrm{i}}$ and $\boldsymbol{\theta}^{\mathrm{i}}$, eqn (24) can be rewritten in a partitioned form:

$$\begin{bmatrix} \mathbf{K}_{uu}^{\mathrm{ii}} & \mathbf{K}_{u\theta}^{\mathrm{ii}} & \mathbf{K}_{uu}^{\mathrm{ic}} & \mathbf{K}_{u\theta}^{\mathrm{ic}} \\ \mathbf{0} & \mathbf{K}_{\theta\theta}^{\mathrm{ii}} & \mathbf{0} & \mathbf{K}_{\theta\theta}^{\mathrm{ic}} \\ \mathbf{K}_{uu}^{\mathrm{ci}} & \mathbf{K}_{u\theta}^{\mathrm{ci}} & \mathbf{K}_{uu}^{\mathrm{cc}} & \mathbf{K}_{u\theta}^{\mathrm{cc}} \\ \mathbf{0} & \mathbf{K}_{\theta\theta}^{\mathrm{ci}} & \mathbf{0} & \mathbf{K}_{\theta\theta}^{\mathrm{cc}} \end{bmatrix} \begin{Bmatrix} \mathbf{u}^{\mathrm{i}} \\ \boldsymbol{\theta}^{\mathrm{i}} \\ \mathbf{u}^{\mathrm{c}} \\ \boldsymbol{\theta}^{\mathrm{c}} \end{Bmatrix} = \begin{Bmatrix} \mathbf{f}^{\mathrm{i}} \\ \mathbf{q}^{\mathrm{i}} \\ \mathbf{f}^{\mathrm{c}} \\ \mathbf{q}^{\mathrm{c}} \end{Bmatrix} \tag{30}$$

where $\mathbf{f}^{\mathrm{i}}$, $\mathbf{q}^{\mathrm{i}}$, $\mathbf{f}^{\mathrm{c}}$ and $\mathbf{q}^{\mathrm{c}}$ are corresponding vectors suitably obtained from eqn (24).

After statically condensing out the interior degrees of freedom $\mathbf{u}^{\mathrm{i}}$ and $\boldsymbol{\theta}^{\mathrm{i}}$, the following equation for the potential contact region can be obtained:

$$[\hat{\mathbf{K}}] \begin{Bmatrix} \mathbf{u}^{\mathrm{c}} \\ \boldsymbol{\theta}^{\mathrm{c}} \end{Bmatrix} = \begin{Bmatrix} \mathbf{f}^{\mathrm{c}} \\ \mathbf{q}^{\mathrm{c}} \end{Bmatrix} - \begin{Bmatrix} \hat{\mathbf{f}}^{\mathrm{c}} \\ \hat{\mathbf{q}}^{\mathrm{c}} \end{Bmatrix}, \tag{31}$$

where

$$[\hat{\mathbf{K}}] = \begin{bmatrix} \mathbf{K}_{uu}^{\mathrm{cc}} & \mathbf{K}_{u\theta}^{\mathrm{cc}} \\ \mathbf{0} & \mathbf{K}_{\theta\theta}^{\mathrm{cc}} \end{bmatrix} - \begin{bmatrix} \mathbf{K}_{uu}^{\mathrm{ci}} & \mathbf{K}_{u\theta}^{\mathrm{ci}} \\ \mathbf{0} & \mathbf{K}_{\theta\theta}^{\mathrm{ci}} \end{bmatrix} \begin{bmatrix} \mathbf{K}_{uu}^{\mathrm{ii}} & \mathbf{K}_{u\theta}^{\mathrm{ii}} \\ \mathbf{0} & \mathbf{K}_{\theta\theta}^{\mathrm{ii}} \end{bmatrix}^{-1} \begin{bmatrix} \mathbf{K}_{uu}^{\mathrm{ic}} & \mathbf{K}_{u\theta}^{\mathrm{ic}} \\ \mathbf{0} & \mathbf{K}_{\theta\theta}^{\mathrm{ic}} \end{bmatrix}, \tag{32}$$

$$\begin{Bmatrix} \hat{\mathbf{f}}^{\mathrm{c}} \\ \hat{\mathbf{q}}^{\mathrm{c}} \end{Bmatrix} = \begin{bmatrix} \mathbf{K}_{uu}^{\mathrm{ci}} & \mathbf{K}_{u\theta}^{\mathrm{ci}} \\ \mathbf{0} & \mathbf{K}_{\theta\theta}^{\mathrm{ci}} \end{bmatrix} \begin{bmatrix} \mathbf{K}_{uu}^{\mathrm{ii}} & \mathbf{K}_{u\theta}^{\mathrm{ii}} \\ \mathbf{0} & \mathbf{K}_{\theta\theta}^{\mathrm{ii}} \end{bmatrix}^{-1} \begin{Bmatrix} \mathbf{f}^{\mathrm{i}} \\ \mathbf{q}^{\mathrm{i}} \end{Bmatrix}. \tag{33}$$

Formally the following expression is obtained for the kth body,

$$\begin{Bmatrix} \mathbf{u}^{\mathrm{c}} \\ \boldsymbol{\theta}^{\mathrm{c}} \end{Bmatrix}^k = [\mathbf{B}]^k \begin{Bmatrix} \mathbf{f}^{\mathrm{c}} \\ \mathbf{q}^{\mathrm{c}} \end{Bmatrix}^k + \begin{Bmatrix} \bar{\mathbf{u}}^{\mathrm{c}} \\ \bar{\boldsymbol{\theta}}^{\mathrm{c}} \end{Bmatrix}^k, \tag{34}$$

where $\mathbf{B} = \hat{\mathbf{K}}^{-1}$ and

$$\begin{Bmatrix} \bar{\mathbf{u}}^{\mathrm{c}} \\ \bar{\boldsymbol{\theta}}^{\mathrm{c}} \end{Bmatrix} = [\hat{\mathbf{K}}]^{-1} \begin{Bmatrix} \hat{\mathbf{f}}^{\mathrm{c}} \\ \hat{\mathbf{q}}^{\mathrm{c}} \end{Bmatrix}. \tag{35}$$

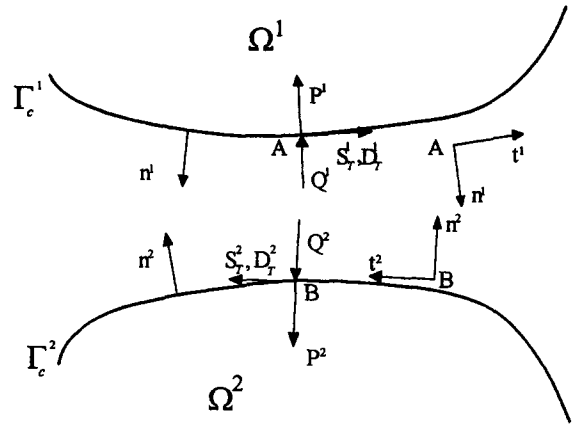

Fig. 2. Principal axes, force, relative displacement and heat flow components at potential contact surface.

Using these relations and the approach in Kwak (1991),

$$\begin{Bmatrix} \mathbf{u}_n \\ \mathbf{u}_t \\ \boldsymbol{\theta} \end{Bmatrix} = \begin{Bmatrix} \mathbf{u}_n^1 + \mathbf{u}_n^2 \\ \mathbf{u}_t^1 + \mathbf{u}_t^2 \\ \boldsymbol{\theta}^1 - \boldsymbol{\theta}^2 \end{Bmatrix} = \begin{bmatrix} \mathbf{B}_{nn} & \mathbf{B}_{nt} & \mathbf{B}_{n\theta} \\ \mathbf{B}_{tn} & \mathbf{B}_{tt} & \mathbf{B}_{t\theta} \\ \mathbf{0} & \mathbf{0} & \mathbf{B}_{\theta\theta} \end{bmatrix} \begin{Bmatrix} \mathbf{P} \\ \mathbf{S}_T \\ \mathbf{Q} \end{Bmatrix} + \begin{Bmatrix} \bar{\mathbf{u}}_n \\ \bar{\mathbf{u}}_t \\ \bar{\boldsymbol{\theta}} \end{Bmatrix} \tag{36}$$

where $\mathbf{B}_{nn} = -\mathbf{B}_{nn}^1 - \mathbf{B}_{nn}^2$, $\mathbf{B}_{nt} = \mathbf{B}_{nt}^1 + \mathbf{B}_{nt}^2$, $\mathbf{B}_{n\theta} = -\mathbf{B}_{n\theta}^1 + \mathbf{B}_{n\theta}^2$, $\mathbf{B}_{tn} = -\mathbf{B}_{tn}^1 - \mathbf{B}_{tn}^2$, $\mathbf{B}_{tt} = \mathbf{B}_{tt}^1 + \mathbf{B}_{tt}^2$, $\mathbf{B}_{t\theta} = -\mathbf{B}_{t\theta}^1 + \mathbf{B}_{t\theta}^2$, $\mathbf{B}_{\theta\theta} = -\mathbf{B}_{\theta\theta}^1 - \mathbf{B}_{\theta\theta}^2$, and the subscripts n and t refer to the normal and tangential axis, respectively. The last term in eqn (36) denotes a suitably obtained vector which is not a function of $(\mathbf{P}, \mathbf{S}_T, \mathbf{Q})$. It can be represented as follows:

$$\begin{Bmatrix} \bar{\mathbf{u}}_n \\ \bar{\mathbf{u}}_t \\ \bar{\boldsymbol{\theta}} \end{Bmatrix} = \begin{Bmatrix} \bar{\mathbf{u}}_n^1 + \bar{\mathbf{u}}_n^2 \\ \bar{\mathbf{u}}_t^1 + \bar{\mathbf{u}}_t^2 \\ \bar{\boldsymbol{\theta}}^1 - \bar{\boldsymbol{\theta}}^2 \end{Bmatrix}. \tag{37}$$

COMPLEMENTARITY FORMULATION AND SOLUTION METHOD

The complementarity formulation of two-dimensional frictional contact derived in Kwak and Lee (1988) is used for the mechanical part. To describe the complementarity in the Coulomb friction law, an incremental relative slip value $\mathbf{D}_T$ at a contact pair is expressed in terms of displacement increments and rigid body motion, and replaced with a difference of two non-negative variables as follows:

$$\mathbf{D}_T \equiv \mathbf{D}_T^+ - \mathbf{D}_T^- \equiv \mathbf{u}_i^1 \mathbf{t}_i^1 + \mathbf{u}_i^2 \mathbf{t}_i^2 - \mathbf{A}_{ij} \boldsymbol{\varphi}_j, \tag{38}$$

$$\mathbf{D}_T^+ \geqslant 0 \text{ and } \mathbf{D}_T^- \geqslant 0, \tag{39}$$

where $\mathbf{t}_i^1$ and $\mathbf{t}_i^2$ are tangential base vector components at a contact point as shown in Fig. 2.

By introducing slack variables $\mathbf{T}^+$ and $\mathbf{T}^-$, eqn (14) can be rewritten as

$$\mathbf{S}_T + \mu \mathbf{P} - \mathbf{T}^+ = 0, \tag{40}$$

$$\mathbf{S}_T - \mu \mathbf{P} + \mathbf{T}^- = 0, \tag{41}$$

$$\mathbf{T}^+ \geqslant 0 \quad \text{and} \quad \mathbf{T}^- \geqslant 0. \tag{42}$$

Then the following complementarity conditions are satisfied:

$$\mathbf{T}^+ \cdot \mathbf{D}_T^+ = 0, \tag{43}$$

$$\mathbf{T}^- \cdot \mathbf{D}_T^- = 0. \tag{44}$$

Similarly, eqn (1) after discretization can be rewritten in the following matrix form introducing slack variables $\mathbf{V}^+$ and $\mathbf{V}^-$:

$$\mathbf{A}_n^T\mathbf{P} + \mathbf{A}_t^T\mathbf{S}_T + \mathbf{H}^T(\mathbf{F}+\mathbf{dF}) + \mathbf{V}^- = 0, \tag{45}$$

$$\mathbf{A}_n^T\mathbf{P} + \mathbf{A}_t^T\mathbf{S}_T + \mathbf{H}^T(\mathbf{F}+\mathbf{dF}) - \mathbf{V}^+ = 0, \tag{46}$$

$$\mathbf{V}^+ \geqslant 0 \quad \text{and} \quad \mathbf{V}^- \geqslant 0. \tag{47}$$

Decomposing rigid body motion $\boldsymbol{\varphi}$ with non-negative variable $\boldsymbol{\varphi}^+$ and $\boldsymbol{\varphi}^-$, the following complementarity conditions are satisfied:

$$\mathbf{V}^+ \cdot \boldsymbol{\varphi}^+ = 0, \tag{48}$$

$$\mathbf{V}^- \cdot \boldsymbol{\varphi}^- = 0. \tag{49}$$

Consider next the heat flow from a hot body to a cold one through an interface between them. The heat balance equation along the potential contact region is given by:

$$\mathbf{Q}^1 + \mathbf{Q}^2 = 0, \tag{50}$$

where $\mathbf{Q}^1$ and $\mathbf{Q}^2$ represent inward heat flows per unit area to each body.

For simplicity in formulation, it is assumed that body 1 is hotter than body 2. Then the total temperature difference, $\mathbf{T}^1 - \mathbf{T}^2$, between a potential contact pair is always greater than or equal to zero if no thermal contact resistance exists. Denote $\mathbf{Q}$ as the heat flow received by body 2 and $\boldsymbol{\Theta}$ as the temperature difference, i.e.

$$\mathbf{Q} = -\mathbf{Q}^1 = \mathbf{Q}^2, \tag{51}$$

$$\boldsymbol{\Theta} = \mathbf{T}^1 - \mathbf{T}^2 = (\tilde{\boldsymbol{\theta}}^1 + \boldsymbol{\theta}^1) - (\tilde{\boldsymbol{\theta}}^2 + \boldsymbol{\theta}^2), \tag{52}$$

where $\tilde{\boldsymbol{\theta}}^1$ and $\tilde{\boldsymbol{\theta}}^2$ represent the temperature of points on the potential contact region of each body at the end of previous thermal loading step, respectively. Then $\mathbf{Q}$ and $\boldsymbol{\Theta}$ are always greater than or equal to zero. Now it is possible to write a complementarity condition for the conventional thermal boundary condition as follows:

$$\mathbf{Q} \cdot \boldsymbol{\Theta} = 0, \tag{53}$$

$$\mathbf{Q} \geqslant 0 \quad \text{and} \quad \boldsymbol{\Theta} \geqslant 0. \tag{54}$$

The thermal variables, however, are not independent of the status of mechanical variables, i.e. gap and contact pressure. Thus it is necessary to consider eqn (53) in conjunction with eqn (13). It is physically argued that $\boldsymbol{\Theta} > 0$ only when $\mathbf{D}_n > 0$ and $\mathbf{Q} > 0$ only when $\mathbf{P} > 0$.

Using eqn (36) and summarizing eqns (12), (38), (40), (41), (45), (46) and (53), a linear complementarity problem is derived as follows:

$$\mathbf{z} = \mathbf{M}\mathbf{w} + \mathbf{r}, \tag{55}$$

$$\mathbf{w}^{\mathrm{T}}\mathbf{z} = 0, \tag{56}$$

$$\mathbf{w} \geqslant 0 \quad \text{and} \quad \mathbf{z} \geqslant 0, \tag{57}$$

where

$$\mathbf{z} = \{\mathbf{D}_{\mathrm{n}}, \quad \mathbf{D}_{\mathrm{T}}^{+}, \quad \mathbf{T}^{-}, \quad \mathbf{V}^{+}, \quad \mathbf{V}^{-}, \quad \boldsymbol{\Theta}\}^{\mathrm{T}}, \tag{58}$$

$$\mathbf{w} = \{\mathbf{P}, \quad \mathbf{T}^{+}, \quad \mathbf{D}_{\mathrm{T}}^{-}, \quad \boldsymbol{\varphi}^{+}, \quad \boldsymbol{\varphi}^{-}, \quad \mathbf{Q}\}^{\mathrm{T}}, \tag{59}$$

$$\mathbf{M} = \begin{bmatrix} -\mathbf{B}_{\mathrm{nn}} + \mu\mathbf{B}_{\mathrm{nt}} & -\mathbf{B}_{\mathrm{nt}} & \mathbf{0} & -\mathbf{A}_{\mathrm{n}} & \mathbf{A}_{\mathrm{n}} & -\mathbf{B}_{\mathrm{n}\theta} \\ \mathbf{B}_{\mathrm{tn}} - \mu\mathbf{B}_{\mathrm{tt}} & \mathbf{B}_{\mathrm{tt}} & \mathbf{I} & -\mathbf{A}_{\mathrm{t}} & \mathbf{A}_{\mathrm{t}} & \mathbf{B}_{\mathrm{t}\theta} \\ 2\mu\mathbf{I} & -\mathbf{I} & \mathbf{0} & \mathbf{0} & \mathbf{0} & \mathbf{0} \\ \mathbf{A}_{\mathrm{n}}^{\mathrm{T}} - \mu\mathbf{A}_{\mathrm{t}}^{\mathrm{T}} & \mathbf{A}_{\mathrm{t}}^{\mathrm{T}} & \mathbf{0} & \mathbf{0} & \mathbf{0} & \mathbf{0} \\ -\mathbf{A}_{\mathrm{n}}^{\mathrm{T}} + \mu\mathbf{A}_{\mathrm{t}}^{\mathrm{T}} & -\mathbf{A}_{\mathrm{t}}^{\mathrm{T}} & \mathbf{0} & \mathbf{0} & \mathbf{0} & \mathbf{0} \\ \mathbf{0} & \mathbf{0} & \mathbf{0} & \mathbf{0} & \mathbf{0} & \mathbf{B}_{\theta\theta} \end{bmatrix}, \tag{60}$$

$$\mathbf{r} = \{\mathbf{D}_{\mathrm{n}}^{0} + \bar{\mathbf{u}}_{\mathrm{n}}, \quad \bar{\mathbf{u}}_{\mathrm{t}}, \quad \mathbf{0}, \quad \mathbf{H}^{\mathrm{T}}(\mathbf{F} + \mathrm{d}\mathbf{F}), \quad -\mathbf{H}^{\mathrm{T}}(\mathbf{F} + \mathrm{d}\mathbf{F}), \quad \tilde{\boldsymbol{\theta}} + \bar{\boldsymbol{\theta}}\}^{\mathrm{T}}, \tag{61}$$

$$\tilde{\boldsymbol{\theta}} = \tilde{\boldsymbol{\theta}}^{1} - \tilde{\boldsymbol{\theta}}^{2}, \tag{62}$$

with the additional constraint described below eqn (54). That is, $\mathbf{D}_{\mathrm{n}}$ and $\boldsymbol{\Theta}$ must be basic at the same time. So are $\mathbf{P}$ and $\mathbf{Q}$.

This linear complementarity problem with additional constraints can be solved by modifying the Lemke's algorithm (Bazaraa and Shetty, 1979). That is, both $\mathbf{P}$ and $\mathbf{Q}$ for a contacting pair of nodes should be kept basic if one of them becomes basic. Similarly this is true for both $\mathbf{D}_{\mathrm{n}}$ and $\boldsymbol{\Theta}$.

NUMERICAL EXAMPLES AND DISCUSSIONS

Two numerical examples are presented to illustrate the procedure and the results compared with those by ABAQUS. In these examples, the bodies are restricted in the direction where temperature difference exists. Thus the effect of temperature can be significant. The dimensional unit of length used in the examples is millimeters.

Example 1 : *a plate between two rigid bodies*

As shown in Fig. 3, a plate of 20×20 mm^2 is in contact at the top and the bottom with rigid bodies. Thus the plate can expand along only the x-direction. It is assumed that there is a thin layer in the middle between the top and the bottom. It maintains its temperature of 100°C. The temperature of the rigid bodies is 0°C. The two sides of the plate are insulated. Young's modulus of the plate is 206 GPa and Poisson's ratio is 0.3. The coefficient of conductivity of the plate is 52 J (s m°C)$^{-1}$. The thermal expansion coefficient of the plate is 1.7×10^{-5} °C^{-1}.

For a finite element analysis, only a quarter of the plate is considered and modeled with 56 quadratic plane strain elements and 199 nodes as shown in Fig. 4.

Ten equal temperature increments are used to solve this example. The contact pressure builds up near the edge of the bottom surface and more rapidly as the friction coefficient is larger as shown in Fig. 5. There appears to be a very sharp increase in contact pressure near the edge. The maximum pressure is sensitive to the magnitude of friction coefficient. The distributions of stick and slip zones are shown in Fig. 6. All contact nodes slide on the contact surface except the origin when $\mu = 0.1$. There is a stick zone near the origin when

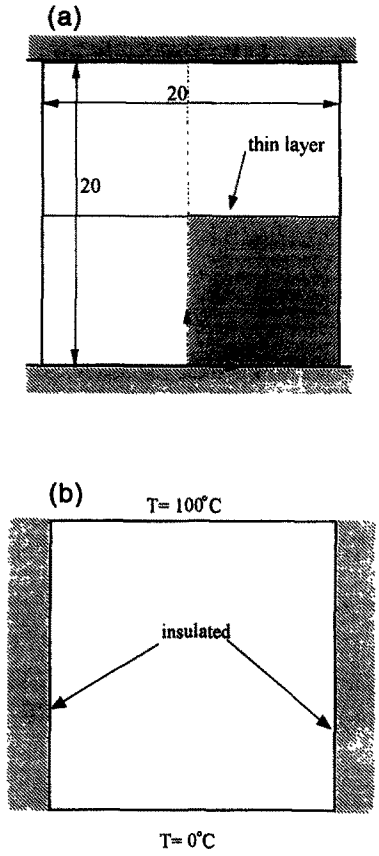

Fig. 3. Geometry of example 1 with (a) mechanical boundary conditions and problem model (hatched), (b) thermal boundary conditions for the problem model.

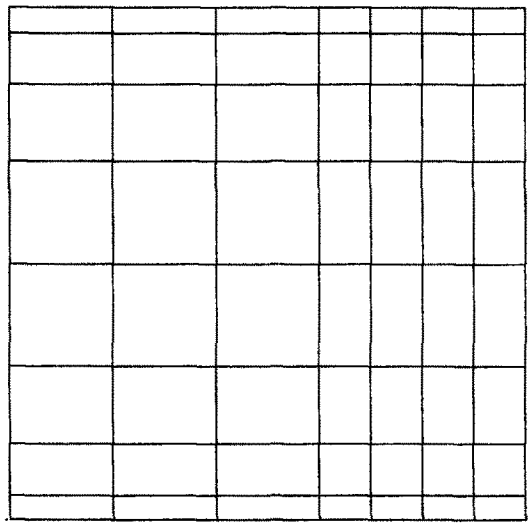

Fig. 4. Finite element model of example 1.

$\mu = 0.3$. Thus the distributions of frictional shear stress near the origin are not proportional to the magnitude of friction coefficient as shown in Fig. 7.

For the results with those by ABAQUS, the temperature–displacement coupled quadratic plane strain element, CPE8T, and the temperature–displacement coupled interface element, INTER3T, are used. ABAQUS uses two different numerical techniques to implement the Coulomb friction model (Hibbitt *et al.*, 1993). One is a penalty method and

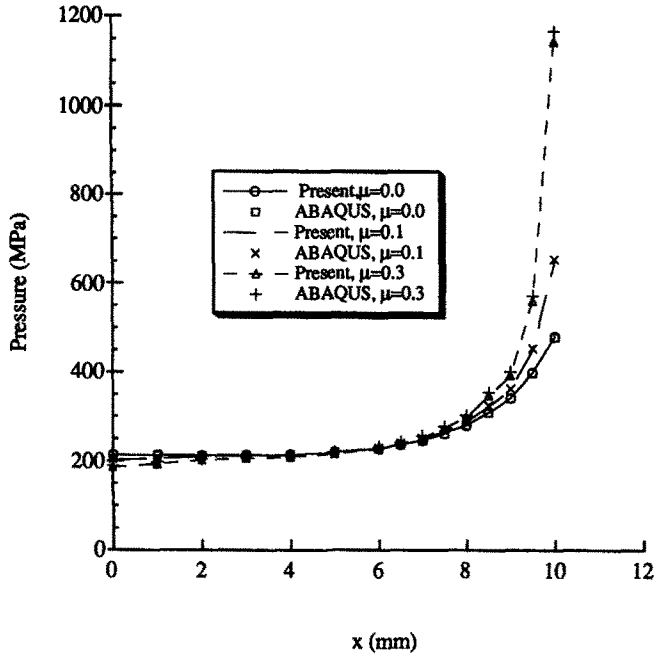

Fig. 5. Pressure distributions along the contact surface of example 1 with various frictional conditions.

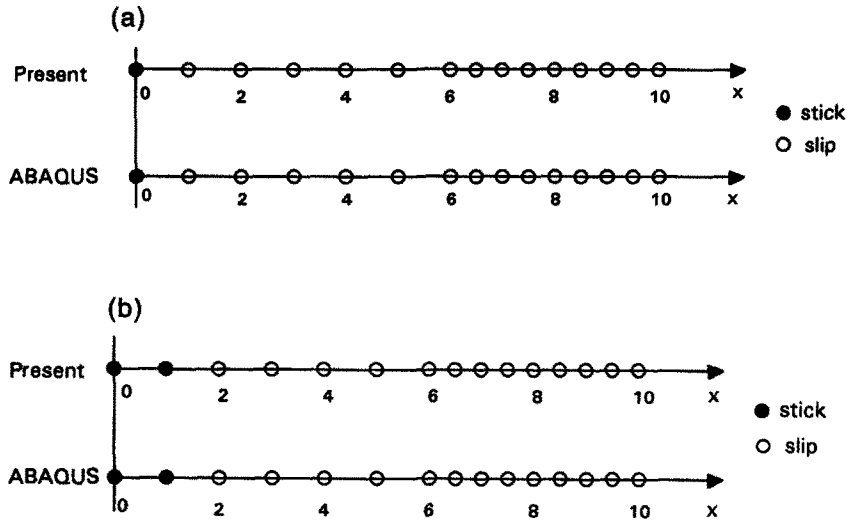

Fig. 6. Distributions of stick and slip zones along the contact surface of example 1 when (a) $\mu = 0.1$ and (b) $\mu = 0.3$.

the other is a Lagrangian multiplier method. To check the stick and slip zones precisely, the keyword card *FRICTION in conjunction with the optional parameter LAGRANGE is used. The results of this example show good agreement with those by ABAQUS.

Example 2: two bodies in contact with the initial gap

Figure 8 shows the geometry with the size in millimeters. An initial gap of 0.05 mm exists between the two bodies before thermal loading. The two sides of body 1 and all faces except the bottom and potential contact region of body 2 are insulated. As the temperature difference between the top of body 1 and the bottom of body 2 increases, the bottom of body 1 touches body 2. Since the conventional thermal boundary condition as previously

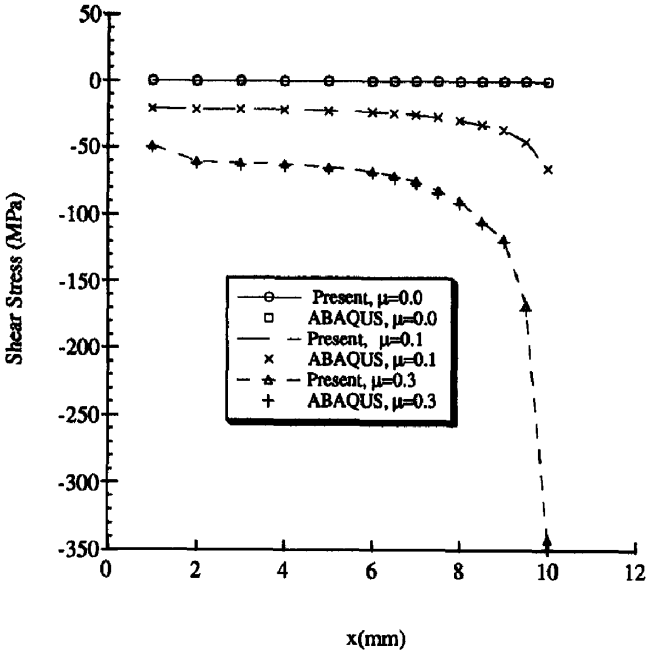

Fig. 7. Frictional shear stress distributions along the contact surface of example 1.

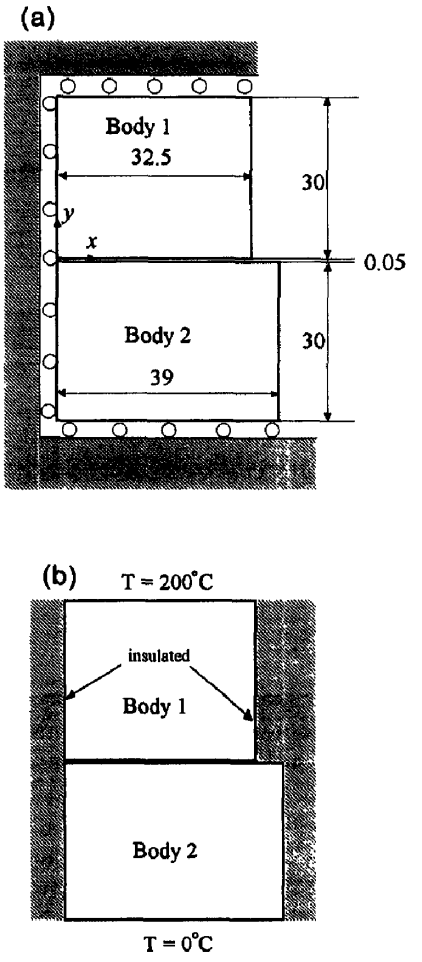

Fig. 8. Geometry of example 2 with (a) mechanical, (b) thermal boundary conditions.

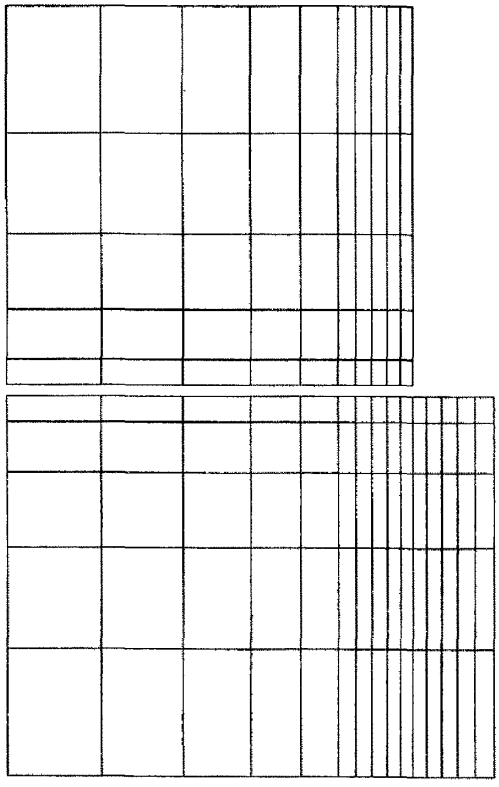

Fig. 9. Finite element model of example 2.

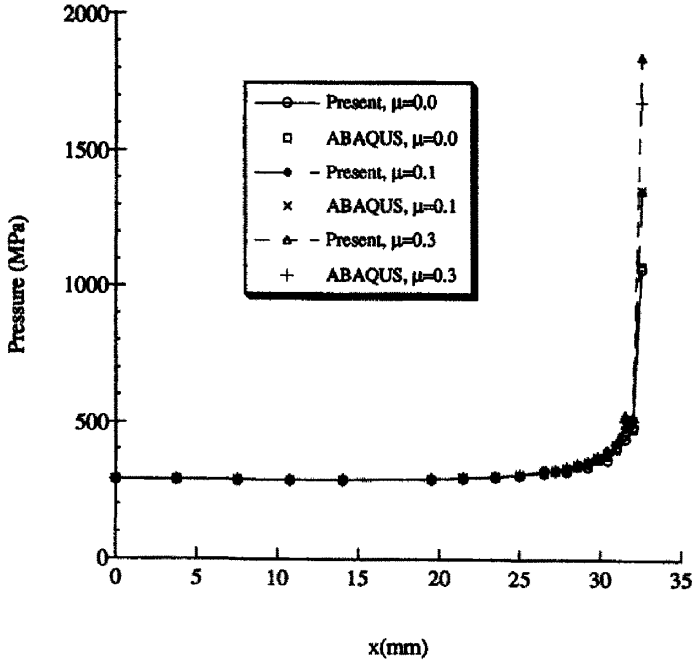

Fig. 10. Pressure distributions along the contact surface of example 2 with various frictional conditions.

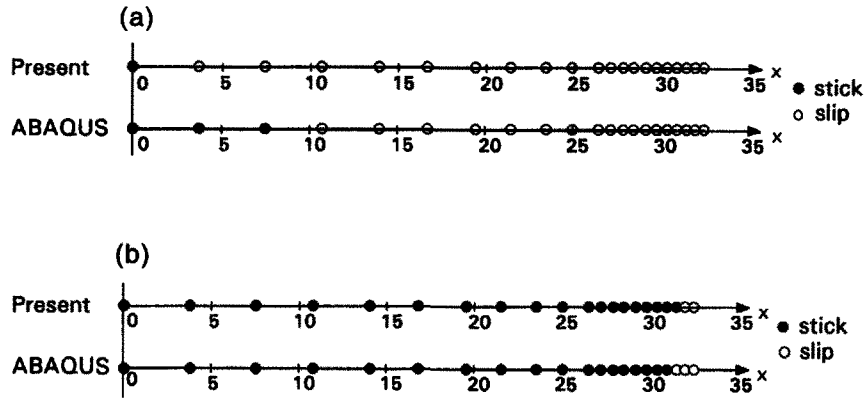

Fig. 11. Distributions of stick and slip zones along the contact surface of example 2 when (a) $\mu = 0.1$ and (b) $\mu = 0.3$.

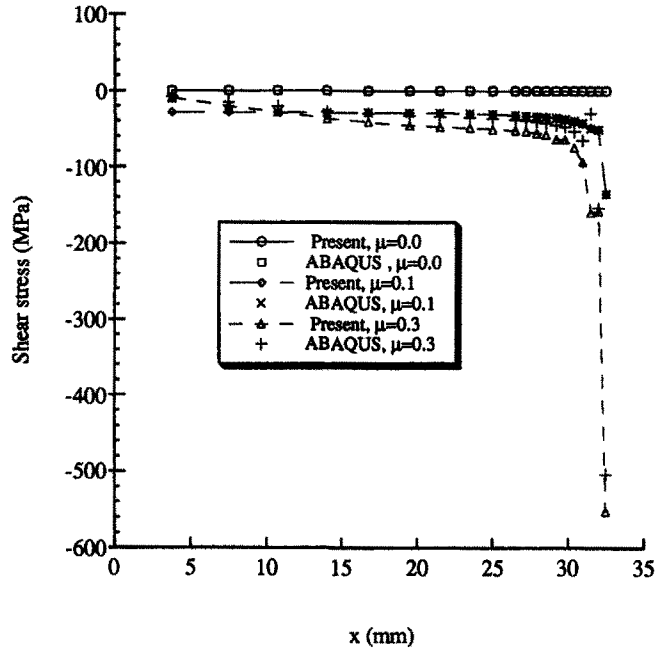

Fig. 12. Frictional shear stress distributions along the contact surface of example 2.

explained is adopted, no heat exchange exists between them before contact. The material properties are the same as the plate of example 1. Body 1 is modeled with 50 quadratic plane strain elements and 181 nodes, and body 2 with 75 quadratic plane strain elements and 266 nodes as shown in Fig. 9.

Ten equal load increments are used to analyse this example. Figure 10 shows the pressure distributions along the contact surface of body 1 with various frictional conditions when the temperature difference is 200°C. The frictional effect to the contact pressure distributions are relatively small as compared to example 1 because the two bodies are allowed to expand laterally. The stick and slip zones obtained from the present method and ABAQUS are somewhat different near the origin when $\mu = 0.1$ and near the edge when $\mu = 0.3$ as shown in Fig. 11. As shown in Fig. 12, the frictional shear stress near the edge is much more wildly distributed in the ABAQUS results than the present when $\mu = 0.3$. The deformed profiles of the top of body 2 with different frictional coefficients are shown in Fig. 13. It is very much influenced by the magnitude of friction coefficient. The same type of elements and keyword cards as in example 1 are used for ABAQUS runs.

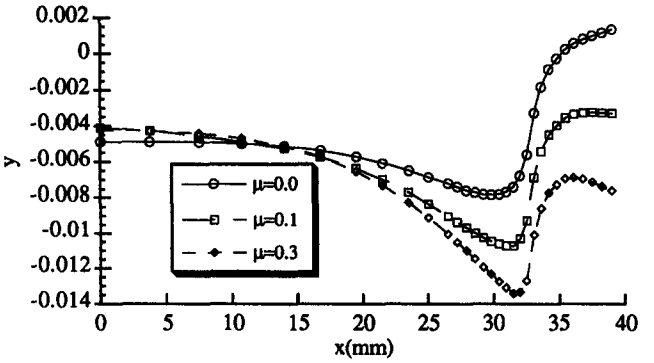

Fig. 13. Deformed profiles of the contact surface of body 2 with various frictional conditions.

CONCLUSIONS

A thermo-mechanical frictional contact is formulated as a linear complementarity problem with additional constraints which is introduced to handle thermal boundary conditions on the potential contact region. A modified Lemke's algorithm is derived to manage the constraints.

Two examples are considered and the results compare very favorably with those by ABAQUS. It is shown that both friction and thermo-mechanical coupling effect can be formally handled by the present method. In these examples, it is known that the distributions of contact stresses, and stick and slip zones are very sensitive to the magnitude of friction coefficient in thermo-mechanical contact.

REFERENCES

Antes, H. and Panagiotopoulos, P. D. (1992). *The Boundary Integral Approach to Static and Dynamic Contact Problems*. Birkhäuser.

Bathe, K. J. (1982). *Finite Element Procedures in Engineering Analysis*. Prentice-Hall, New Jersey.

Bazaraa, M. and Shetty, C. M. (1979). *Nonlinear Programming: Theory and Algorithms*. John Wiley, New York.

Carter, J. P. and Booker, J. R. (1989). Finite element analysis for coupled thermoelasticity. *Comput. Struct.* **31,** 73–80.

Chandrasekaran, N., Haisler, W. E. and Goforth, R. E. (1987). A finite element solution method for contact problems with friction. *Int. J. Num. Meth. Engng* **24,** 477–495.

Comninou, M., Dundurs, J. and Barber, J. (1981). Planer Hertz contact with heat conduction. *ASME J. Appl. Mech.* **48,** 549–558.

Duvaut, G. and Lions, J. L. (1976). *Inequalities in Mechanics and Physics*. Springer, New York.

Hibbitt, Karlsson and Sorensen Inc. (1993). *Note on Contact and Friction Analysis with ABAQUS*.

Holman, J. E. (1986). *Heat Transfer*. McGraw-Hill, New York.

Klarbring, A. (1986). General contact boundary conditions and the analysis of frictional systems. *Int. J. Solids Structures* **22,** 1377–1398.

Kwak, B. M. (1990). Numerical implementation of three-dimensional frictional contact by a linear complementarity problem. *KSME J.* **4,** 23–31.

Kwak, B. M. (1991). Complementarity problem formulation of three dimensional frictional contact. *ASME J. Appl. Mech.* **113,** 134–140.

Kwak, B. M. and Lee, S. S. (1988). A complementarity problem formulation for two dimensional frictional contact problems. *Comput. Struct.* **28,** 469–480.

Mahmoud, F. F. and El Shafei, A. G. (1989). A direct automated procedure for frictionless thermoelastic contact problems. *Engng Fract. Mech.* **33,** 157–164.

Montmitonnet, P., Chenot, J. L., Bertrand-Corsini, C., David, C., Iung, T. and Buessler, P. (1992). A coupled thermomechanical approach for hot rolling by a 3D finite element method. *ASME J. Engng Ind.* **114,** 336–344.

Panagiotopoulos, P. D. (1975). A nonlinear programming approach to the unilateral contact and friction boundary value problem in the theory of elasticity. *Ing. Archiv.* **44,** 421–432.

Panagiotopoulos, P. D. (1985). *Inequality Problems in Mechanics and Applications*. Birkhäuser.

Panek, C. and Dundurs, J. (1979). Thermo-elastic contact between bodies with wavy surfaces. *ASME J. Appl. Mech.* **46,** 854–860.